Journal of Remote Sensing & GIS
ISSN: 2469-4134

Alegria et al., J Remote Sensing & GIS 2017, 6:2
DOI: 10.4172/2469-4134.1000197

Research Article Open Access

# Hazard Mapping of Landmines and ERW Using Geo-Spatial Techniques

**Aura Cecilia Alegria[1,2*], Esteban Zimanyi[2], Jan Cornelis[1] and Hichem Sahli[1,3]**

[1]Department of Electronics and Informatics (ETRO), Vrije Universitit Brussel, Pleinlaan 2, 1050 Brussels, Belgium
[2]Department of Computer and Decision Engineering (CoDE), Universitit Libre de Bruxelles, Avenue FD Roosevelt 50, Brussels, Belgium
[3]Interuniversity Microelectronics Centre (IMEC), Kepeldreef 75, Heverlee, Belgium

## Abstract

Landmines and Explosive Remnants of War (ERW) continue to represent a significant nuisance for society in affected countries. Coping with humanitarian and development activities, mine action aims at both, reducing the impacts of the presence of landmines/ ERW on the population, and ultimately returning cleared land to the communities. These are the main tasks of mine action decision makers. This study combines landmine/ERW contamination data with explanatory variables that contain information about underlying targets. They are integrated into a risk mapping framework using Geographic Information Systems with other information sources, such as remote sensing. The aim of this paper is to provide insights into the populations and/or locations at risk caused by landmine and ERW impacts on a broad and local scale. Thus, the concept of 'hotspots' is particularly useful because it provides a visual representation of exposure, aided by a geo-spatial representation of 'priority areas for mine action planners to focus on. We apply the Kernel Density Estimator (KDE) to derive such 'hotspots'. KDE is proposed as the basis to define landmine and ERW hazard, vulnerability, and element-at-risk maps, which enable producing a final output, the landmine/ERW risk map. This is accomplished by using an adaptive kernel bandwidth for datasets with highly heterogeneous spatial distributions, and a problem specific method for generating point samples from polygon data, before using them as inputs for KDE. The geo-statistical model presented here is a time-and-cost-efficient method to construct a landmine risk map, that is as representative as those produced by mine action actors. It can be used as a complement to the risk area maps made by these actors because they are slightly different but show a large degree of overlap. Moreover, the method helps revealing the variables which are the most linked to landmine/ERW-related events in the study area.

**Keywords:** Humanitarian mine action; Landmine risk; Risk indicators; Risk mapping; Geo-Spatial models; KDE

## Introduction

Landmines and other Explosive Remnants of War (ERW) are an enduring legacy of conflicts [1]. Mines and ERW-impacted areas threaten the subsistence of their inhabitants by denying them the access to vital resources such as forests, agricultural land, pasturage, and water [2]. Thus, landmines and ERW propagate socio-economic underdevelopment and environmental degradation long time after their military purposes have been served.

In this paper, a risk mapping framework is proposed. Definitions of risk are commonly probabilistic in nature, "referring to the potential losses from a particular hazard to a specified element at risk in a particular time" [3]. Landmine and ERW risk is the probability of harmful consequences or likelihood of losses resulting from interactions between: (i) landmine and ERW hazards, i.e., the occurrence of landmine or ERW events; (ii) element at risk, i.e., population, its livelihoods and assets in an area in which landmine or ERW events occurred; and (iii) vulnerability, i.e., the susceptibility of exposed elements to suffer adverse effects when impacted by landmine and ERW events. Expressed in another way, risk, $R$, is determined by [3]:

$$R=V\cdot E\cdot H. \quad (1)$$

where $V$ is the vulnerability, $E$ is the cost or amount of the 'element at risk', and $H$ is the hazard probability.

This paper explores the Kernel Density Estimator (KDE) to define landmine and ERW hazard, vulnerability, and element at risk. Since the aim is to provide insights into the populations and/or locations at risk to landmine and ERW impacts both on a broad and local scale, the concept of 'hotspots', is particularly useful. Thus, we apply KDE to derive 'hotspots'. They provide a visual representation of exposure aided by a geo-spatial representation of 'priority areas' for mine action planners to focus on.

The paper is organized as follows. Section 4 introduces the terminology and standard processes used in Humanitarian Mine Action (HMA). Section 5 presents mine action data, as well as commonly used explanatory data. To estimate landmine and ERW threats in affected countries, Section 6 details the proposed risk mapping methodologies, namely, KDE and the risk analysis framework to investigate possible factors linked to the risk generated by landmines and ERW. Each approach achieves a different objective, for instance:

(i) KDE helps estimating the landmine/ERW hazard density. It allows discovering variations in contamination density, and helps visualizing at-risk populations; and

(ii) The risk analysis framework with its three components: hazard, vulnerability and element at risk [4] helps in discovering the risk-prone areas under the presence of certain risk indicators, and social, economic and environmental conditions. This allows evaluating the risk on populations, the impact on populations (with socio-economic considerations) and the impact on infrastructures.

In Section 7 we illustrate the proposed methodology using data-sets from Bosnia and Herzegovina (BIH). Finally, in Section 8 we draw some conclusions and a discussion of the use of the proposed maps.

***Corresponding author:** Aura Cecilia Alegria, Department of Electronics and Informatics (ETRO), Vrije Universitit Brussel, Pleinlaan 2, 1050 Brussels, Belgium, Tel: 3226292986; Fax: 3226292883; E-mail: aalegria@vub.ac.be

**Received** April 27, 2017; **Accepted** May 12, 2017; **Published** May 15, 2017

**Citation:** Alegria AC, Zimanyi E, Cornelis J, Sahli H (2017) Hazard Mapping of Landmines and ERW Using Geo-Spatial Techniques. J Remote Sensing & GIS 6: 197. doi: 10.4172/2469-4134.1000197

**Copyright:** © 2017 Alegria AC, et al. This is an open-access article distributed under the terms of the Creative Commons Attribution License, which permits unrestricted use, distribution, and reproduction in any medium, provided the original author and source are credited.

## Background on Humanitarian Mine Action

The international response to the landmine and ERW problem is referred as Humanitarian Mine Action (HMA). HMA is defined as the set of "activities which aim to reduce the social, economic and environmental impact of mines and ERW including unexploded sub-munitions" [5]. Compared to other humanitarian actions, mine action activities are 'standardized'. Indeed, the International Mine Action Standards (IMAS) have been defined under the United Nations Mine Action Service (UNMAS), and currently continuously revised by the Geneva International Centre for Humanitarian Demining (GICHD). GICHD is also the developer and maintainer of the Information Management System for Mine Action (IMSMA), being a GIS-based information system to manage all data concerning HMA activities.

HMA activities normally start with a task known as 'impact survey' which is defined as "an assessment of the socio-economic impact caused by the actual or perceived presence of landmines and ERW, in order to assist the planning and prioritisation of HMA programmes and projects" [5]. The impact survey is the process by which a comprehensive inventory of: (i) topographic information (both natural and man-made features such as land-cover, populated areas, transportation routes and facilities, and other features such as hospitals, among others); and (ii) contamination information. The contamination information is of two types: (i) all locations of known mine accidents/incidents, and (ii) all reported or suspected locations of mines or ERW and Unexploded Ordnance (UXO) contamination, denoted as Suspected Hazardous Areas (SHA) [5]. Generally, an SHA does not have a precisely known perimeter, only a location and an estimated quantity of landmines and ERW. An SHA could also represent a known laid minefield; in such a case, it is represented by either a location and estimated number of landmines and ERW, or as a polygon (minefield extent), contamination type, and if available, the minefield pattern.

The collected mine action data, being mine incidents/accidents (point data), minefield records (point or polygon data), and SHA (point or polygon data), are generally entered in a mine action information database, such as IMSMA, for further use. This information allows assessing the impact of the landmine and ERW problem on the affected areas both at local and global (country) levels. The landmine impact is a simple scoring rule estimated as a weighted sum of 13 variables which includes the number of recent victims, certain livelihood and institutional blockage variables (access to roads, cultivated area, rivers among others) characterizing the mine affected community under study, and binary variables indicating whether mines or UXO have been present. The mine impact score system permits a classification of the mine affected communities into three classes: 'Low', 'Medium' and 'High'. The working hypothesis is that communities scoring high are most likely the ones in which HMA has the greatest potential for reducing future suffering.

Starting from SHAs, identified through the impact survey, the land release process [6] is as follows. First, a non-technical survey is done on an SHA to define the borders of one or several Confirmed Hazardous Areas (CHAs) where the presence of mine/ERW contamination has been confirmed on the basis of direct evidence. CHAs are normally represented as polygons, and generally include information about the suspected type of contamination, topography, access, vegetation, and potential economic use of the area after clearance. Parts of the SHA that are not included in the CHAs are called cancelled areas. The second step, the technical survey, allows identifying and delineating, within a CHA, one or several Defined Hazardous Areas (DHAs), represented as polygons. The CHA can be released, while the DHA require full clearance. In the remaining part of this work, we will use the term hazardous area, as a generic term for an area perceived to have landmines and/or ERW (SHA, CHA, DHA) [6].

## Landmines and ERW Risk Indicators: Explanatory Variables

Since the work of [7], space and airborne survey including Unmanned Aerial Vehicle (UAV) have demonstrated the usefulness of remote sensing to collect visible indicators of landmines and ERW in a contaminated area. Landmines and ERW risk indicators represent two-dimensional object features which are signs of landmine/ERW deployment in its proximity. Many of these indicators can be identified through visual inspection or image analysis of remote sensing imagery [8-10]. The picture in Figure 1 illustrates some indicators that were collected with the aid of an UAV during the SAFEDEM feasibility study in 2011 in Bosnia and Herzegovina.

Building ruins, craters and holes, and destroyed military equipment are some of such indicators. Such indicators are often represented as point data. Supported by the idea of using approaches based on land-cover/land-use change detection that involve historical images, the following items could be considered as remnants of war indicators [11]: tracks that are no longer in use, abandoned agriculture/pasture areas, and edges of forests. Such indicators are often represented as polygons.

In order to construct a geo-statistical model for landmine risk mapping, we first need to define a set of explanatory variables that capture the relationship between the spatial pattern of the target variable (landmine incidents, hazard areas, minefields) and the surrounding geographic area. The following variables are often considered [12]:

- Digital elevation model, which allows estimating elevation and slope information for characterizing the topography of the area.
- Land-cover and land-use, which are linked to the socio-economic development or blockage of a mine affected area. The five main used categories are built-up areas, agricultural areas, forests/semi-natural areas, wetlands, and water bodies.
- Roads, railways, trails, tracks and paths, being the most commonly used means of transportation for people and goods. They give access to work places, educational centres, service facilities such as hospitals, government offices, and other sites. Frequently, their blockage is used as an inhibition for freedom of movement.

**Figure 1:** UAV image showing a building ruin with ERW devices.

- Rivers, which are a source of fishing, transportation and other activities, such as irrigation.
- Buildings, which are commonly gauges of permanent human activity.

## Methods for Landmines and ERW Risk Mapping

### Kernel density estimation

KDE [13] is a non-parametric method that enables the quantification of the extent of a given spatial phenomenon. Maps generated applying KDE have been widely used to analyze and visualize spatial distributions of discrete presence or counts data, which are represented as point locations, but also for identifying hotspots [14]. The choice of using KDE is based on the observation that the risk coming from a known incident gets lower by increasing the distance to its location. This idea agrees with Tobler's first law of geography: "Everything is related to everything else, but near things are more related than distant things" [15]. KDE has been widely applied in domains such as seismic hazard analysis [16], crime mapping [17], public health control [18], public transport [19], environmental risks mapping [20], biomass [21], and wildlife home range estimation [22,23], among others.

In the case of landmine and ERW risk mapping, KDE helps in: (i) visualising administrative divisions where highest concentrations of landmine/ERW are located (also known as hotspots), (ii) visualizing at-risk populations through maps that combine landmine/ERW hazards and population data (population at risk=Presence of population × Presence of hazards), (iii) examining possible relations with transportation features (e.g., near roads), and (iv) understanding the dynamics of the contamination in the case of temporal data. In a previous work [24], the application of KDE was explored as an approach to analyze variations in mine incidents density. In Ref. [11], it was further investigated the analysis as part of a GIS-based weighted linear combination approach, where points, lines and polygon-shaped variables were modelled as the result of a KDE mapping. The concept has been further enriched by Ref. [25] by considering highly heterogeneous spatial distributions, and also by considering the use of non-point data such as polygons. For polygon data such as SHAs, Ref. [25] proposed infilling the polygons with points before using them as inputs in the kernel density estimation. The authors pointed out that mapping using KDE applied to points and centroids of polygons "can be used to show more details, is less sensitive to the Modifiable Areal Unit Problem (MAUP), preserves areas of low contamination, stores data at the national level and is likely to encourage the sharing of information". In this work, we use the same idea; however, we propose a new approach for sampling points within polygons representing mine field polygons and Hazard Areas. KDE is a suitable method for summarizing and visualizing the underlying properties of point patterns. It can be used to estimate the density at any location in the study area and to transform the spatial points into a continuous 3D surface. The approach consists in dividing the study area into regular grid cells and estimating a density value for each grid cell according to the selected characteristics of the spatial points. In addition, quantitative analysis can be applied based on these grid cells. The density value can be estimated by the formula:

$$f(\mathrm{X}) = \frac{1}{nh}\sum_{i=1}^{n} K\left(\frac{X_i - X}{h}\right) \quad (2)$$

were $f(X)$ is the density value at a location $X$ of the grid cell with coordinates $(x,y)$, $n$ the number of observations (events), $X_i(x_i,y_i)$ the given observation points, $h$ the bandwidth and $K(u)$ a kernel (density) function. In this work, the Gaussian kernel function is chosen, $K(\mathrm{u}) = \frac{1}{\sqrt{2\pi}}\exp^{-\frac{u^2}{2}}$. As it can be observed in Equation (2), the KDE function is dependent on an arbitrarily specified bandwidth size. Several statistical methods have been suggested to find an optimal bandwidth, such as Likelihood Cross Validation (LCV), Least Squares Cross Validation (LSCV), Biased Cross Validation (BCV) and Smoothed Cross Validation (SCV) [26-29], among others. Bandwidth selection has a significant effect on the visualization of landmine and ERW events [24,25]. In [25], the bandwidth was adjusted to the input data using a user-defined parameter. The authors select the bandwidth as the average distance to the *k-th* nearest neighbour, with $k$=round $\left[\sqrt{n.p}\right]$, where $n$ is the number of points and $P$ is a user-provided parameter to adjust the detail level of the map. The parameter $k$ "reflects the degree of clustering and the spacing of points, rather than the extent of the study area or the point dataset size" [25].

In this study, we adopt the adaptive bandwidth approach given that it has the advantage of providing constant precision for the estimate over an entire region. Indeed, as also mentioned in Ref. [30], in situations where the risk is more concentrated in rural regions, as is the case for landmines and ERW related risk (e.g., due to sparse data), the adaptive risk estimator benefits from variance stabilization when it is compared to the fixed bandwidth approach. In our implementation, the adaptive bandwidth method of the sparr R-package [31] has been used. It adopts the bivariate Gaussian kernel function. The adaptive smoothing is calculated by using Abramson's method [32]. In this approach, for each point data location $X_i$, the bandwidth $h(i)$ is given by:

$$h(i)=h_0 f(X_i)^{-1/2}\gamma^{-1}. \quad (3)$$

where $h_0$ is a secondary smoothing multiplier known as the global bandwidth, and $\gamma$ is the geometric mean of the $f(X_i)^{(1/2)}$ terms, serving to alleviate the dependency on the scale of the recorded data. This formulation is quite natural since the amount of smoothing depends inversely on the local amount of data. The unknown $f(X_i)$ should be replaced by a pilot density, which in its turn is a fixed bandwidth kernel density estimate constructed with a pilot bandwidth $h$. More details are found in Ref. [13].

**Dual KDE:** Even if the KDE approach can be used for a wide range of tasks, in some situations knowing the spatial distribution is not enough. Indeed, when dealing with risk it is useful to analyse the locations distribution with respect to another 'factor', for example the underlying population. The secondary factor can be represented as point or linear features. The first case occurs, for example, when one is interested in analysing locations of a disease against the urban centres which are represented as points, as in Ref. [33]. The second case is used, for example, when analysing traffic accidents along streets as in Ref. [34]. Dual KDE is a good approach to reveal differing or similar patterns between two different geographic distributions, allowing a more succinct interpretation. It is obtained by producing a density surface that depicts the estimations for the relationship between the two considered variables, expressed as a continuous surface [35]. These estimates are calculated by overlaying a grid covering the study area, in which the distance from each cell to every point within a specified distance is measured and weighted based on its proximity to the cell origin. The overlay between the two densities can materialize any mathematical expression representing the desired relationship. For instance, in Ref. [36], the authors subtract the 'typical' (or average) total

crime value, from the 'high period' (i.e., with the biggest crime scores) crime value, to represent changes between the 'typical' daily crime values and the 'highest' daily crime values. When dealing with risk related topics, the natural logarithm of the density ratio is an advised choice [37]:

$$\text{Log ratio of densities} = Ln[f(x_j)/g(y_j)] \quad (4)$$

where $f(x_j)$ is the KDE for the primary set of locations points and $g(y_j)$ is the KDE for the secondary set, both $f(x_j)$ and $g(x_j)$ are estimated as explained earlier in Section 6.1. The log ratio is used for cases where a variable is spatially skewed, such that most reference cells have very low density estimates, while a few have very-high density estimates. Converting the ratio into a log function will tend to attenuate the spikes that occur. In this study, we use the dual KDE to produce maps which are used to represent vulnerable areas as it will be detailed in Section 6.2.

## Disaster risk analysis

The concept of spatial risk has been traditionally linked to natural sources, such as cyclones, droughts, floods, earthquakes, volcanoes, landslides, among others [38].

In this work, we adopt the approach proposed in Ref. [3] to quantify the risk $R$ (see Equation 1 in Section 3). Examples of applications using such principle are listed in Table 1, along with the used hazard, vulnerability, and element-at risk parameters. In the following sections, we detail the proposed approach for calculating hazard, vulnerability, and element at risk, for landmine and ERW risk mapping. The final risk map is calculated as the product of the unity-based normalization (i.e., scaling in the range from 0 to 1) of each component.

**Hazard:** In general, a hazard is defined as "a dangerous phenomenon, substance, human activity or condition that may cause loss of life, injury, or other health impacts, property damage, loss of livelihoods and services, social and economic disruption, or environmental damage" [43]. Hazards are described quantitatively by the likelihood frequency of occurrence of different intensities for different areas, as determined from historical data or data analysis, and they are expressed as probabilities. Some studies used KDE as a method to estimate hazard. For example, [20] conducted a risk assessment of environmental toxins by incorporating the kernel density approach for the visualization of varying densities within the study region. The authors used KDE to analyse the spatial distribution of the risk-related scores of 53 facilities subject to the Toxic Release Inventory (TRI) program, to assess the individual chemical releases, the relative toxicity and proximate populations.

In our study, the hazard generated by landmines and ERW expresses the probability of finding an incident, minefield or hazard area in a certain region. We use the KDE-based map as basis to identify areas where landmine and ERW hazards are likely to occur. The data used in this study to create hazard maps consist of (i) landmines and ERW incidents/accidents, represented as points, (ii) minefields, represented as points or polygons, and (iii) hazardous areas represented as polygons. To apply KDE, the polygon data should be transformed to point data. This can be done by reducing the polygons to their respective centroids before applying the KDE procedure. Such approach does not take into account the distribution/number of the events (being landmines and/or ERW) within the polygon. To obtain a representation closer to reality, we propose filling each polygon $p$ with $N_p = A_p.d_{PD}$ random points, with $A_p$ the area of the polygon $p$ in $km^2$ and $d_{PD}$ the density of the mine action point data within the 'very-high risk' area. Here, the density, $d_{PD}$, is defined as the number of points/km$^2$, obtained as follows. Let $PD$ denote the set of all reported incidents/accidents and minefield points, within the study region. We first apply KDE on $PD$, then we classify five categories of hotspots, using the Jenks natural breaks classification [44]. Natural-breaks are designed to determine the best arrangement of values into different classes according to their statistical characteristics; it requires an iterative process that seeks to minimize the variance within classes and maximize the variance between classes [44]. The method is extensively applied to classify and visualize geographic data. We chose this method to classify the grid cells of the KDE density surface into five (5) Class Num classes, and label each grid cell using the corresponding Class Num to indicate the strength/severity of the hazard of the grid cell. The considered five classes are denoted as very-high, high, medium, low and very-low. Within the top category (denoted as 'very-high risk') we count the number, N, of points as concentrations of exceptional vulnerability. Finally, $d_{PD} = N/A$, $A$ being the area covered by of the 'very-high risk' category, expressed in $km^2$. The final hazard map is obtained by applying KDE on a set of points, denoted as $TP$, consisting of the above defined $PD$ data augmented with randomly generated points within 200-meter buffers for $PD$, mine field polygons and hazard area polygons.

**Vulnerability:** In general, vulnerability is "the condition determined by physical, social, economic and environmental factors or processes, which increases the susceptibility of a community to the adverse impact of a hazard" [45]. Vulnerability can be calculated in the form of a vulnerability index ($V\ I$), as the average of all the different type of vulnerabilities e.g., social vulnerability, physical vulnerability and environmental vulnerability [40]. The increasing or decreasing

| Risk | References | Hazard layer | Vulnerability layer | Element-at-risk layer |
|---|---|---|---|---|
| **Malaria** | [39] | Elevation, slope, distance to breeding sites and to streams and wetness index | Distance to health facilities per population index | Reclassified land use or land cover image file on the basis of malaria susceptibility |
| **Petroleum fire** | [40] | Intensity (amount of storage of each petroleum material) X Probability (no. of storage in each ward) / Area | SV (Social Vulnerability)+PV (Physical Vulnerability)+EnV (Environmental Vulnerability)+ECV (Economical Vulnerability)+CIV (Critical Infrastructure Vulnerability) | Population / Area |
| **Natural and man-made hazards** | [41] | Storm, earthquake, flood, man-made hazard | Population, assets, lifelines | Faults, vegetation, topography, toxic sites, nuclear facilities, terrorism hot spots |
| **Landslides** | [42] | Lithology, faults, altitude, slope, land-cover, road network, hydrography, geomorphology, maximum daily precipitation, peak ground acceleration, physical geography | Regions, districts communities | Buildings, population, roads, pipelines, crops, forests, protected areas |

**Table 1:** Applications of risk quantification.

vulnerability index indicates susceptibility of community for one particular hazard. Several possibilities are available for the estimation of the vulnerability. For example, it can be quantified by using methods which refer to the susceptibility of the element at risk (e.g., people or houses) with respect to the hazard [46]; this method requires detailed measures of the extent of the involved elements, which is often very limited. For estimating vulnerability, Ref. [47] involves the use of multicriteria analysis, weighting and summing up factors such as distance to services, infrastructure, and population density. Ref. [48] uses a GIS-based method with the different themes that constitute the Corine Land Cover inventory of the study area to perform the environmental vulnerability assessment to volcanic ash-fall. In our study, we quantify vulnerability as:

$$VI = PV.EnV \tag{5}$$

where $PV$ is the physical vulnerability and $EnV$ is the environmental vulnerability.

The physical vulnerability (PV) is expressed in terms of exposure to unsafe conditions. The population within the study region which is found to be dangerously close to the potential sources of threat, being landmine and ERW, is considered as physically vulnerable. As we do not have population information, in our implementation, the $PV$ is the resulting map of a dual KDE map, contrasting the mine action point data $TP$, against building (or cultivated areas) locations. The environmental Vulnerability (EnV) is defined as potential for environmental degradation due to the existence of a hazard. In our case, it can be calculated as the amount of abandoned land per area unit, for zones with different hazard levels. As measure of abandoned land, we use the vegetation changes information obtained using remote sensing data [11]. The $EnV$ is obtained using dual KDE, contrasting the mine action point data $TP$, against centroids of zones with vegetation changes (or risk indicators points).

**Element at risk:** In general, the element-at-risk factor includes persons, animals, infrastructures and activities in a particular area, that may be adversely affected (directly or indirectly) by the analyzed hazard. The choice of the element-at-risk factor depends on the objectives of the risk assessment, and the available information.

The amount of element at risk, can be quantified either in numbers (of buildings, people, among others), in monetary value (replacement costs, market costs and so on), in area, or in perception (importance of element at risk) [4].

In this study, the considered element-at-risk factor is the population, represented as built-up area from the land-use data. When such information is not available, we use cultivated area as factor representing the impact of landmines and ERW hazards on the agricultural activity. For the estimation of the element-at-risk map, E, we follow the hazard index method as defined in [4]. The method is based on map crossing of two maps denoted as DensMap and DensClas, respectively. DensMap represents the density of events within the area covered by the top hazard categories (i.e., very-high, high, medium) as obtained in Section 6.2.1. Here events denote the set of points used to generate the hazard map, consisting of the mine action point data $TP$, as described in Section 6.2.1. DensClas is a distance to build-up area parameter class map obtained as follows: we first create a raster map defining for each cell the distance to build-up area (or cultivated area). The distances are then grouped, with natural-breaks, into five distance-to-built-up (or distance-to-cultivated) classes. Finally, for each of the five distance classes, DensClas is estimated as the density of events within the area covered by the class, which is in turn assigned to each cell within the class. Finally, the element-at-risk map is obtained as:

$$E = \ln\left(\frac{DensClas}{DensMap}\right) \tag{4.5}$$

## Results and Discussion

### Study area

This paper analyzes two distinct mine-affected areas in Bosnia and Herzegovina (BIH). BIH has been heavily contaminated with mines and ERW as a result of the 1992-1995 conflict related to the break-up of the former Yugoslavia. In Southern and central BIH, mines were often used randomly, with few minefield records kept. According to BHMAC, the total suspected area at the end of 2013 was 1,218.5 km$^2$ or 2.4% of the total area of BIH. There are 19,185 minefield records in the database, which is estimated to represent merely about 60% of their total number. A general assessment of the mine situation in BIH identified 1,417 communities that have been affected by mines, of which 136 communities were at high risk [49]. The BHMAC data information system and the diversity of environmental conditions make BIH a suitable study area for the application of the risk assessment approach proposed in this work.

The data used for the analysis were collected during two projects: the SAFE- DEM feasibility study during 2013-2014. Two study areas have been considered. The first study area is situated in the Dolac municipality in BIH (see Figure 2). A minimum bounding rectangle covering approximately 14.3 square kilometres between coordinates 44°28'N and 44°30'N and 18°08'E and 18°11'E demarcated the area. It is a region irrigated by the Bosna river, with a mean elevation of 326 m (standard deviation of 103 m).

The second study area is situated in the Hadzici municipality in BIH (see Figure 3). A minimum bounding rectangle covering approximately 436 square kilometres between coordinates 43°43'N and 43°53'N and 18°07'E and 18°28'E demarcates the area. The landscape of the region is very rugged, characterized by a mean elevation of 849 m (standard deviation of 330 m).

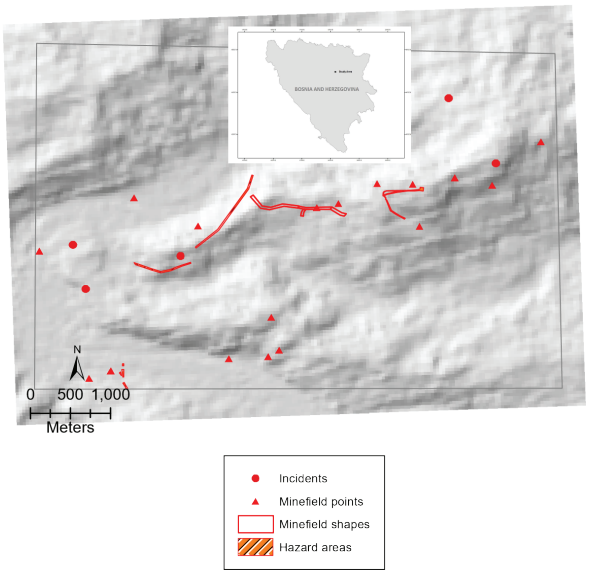


**Figure 2:** Dolac study area in Bosnia and Herzegovina.

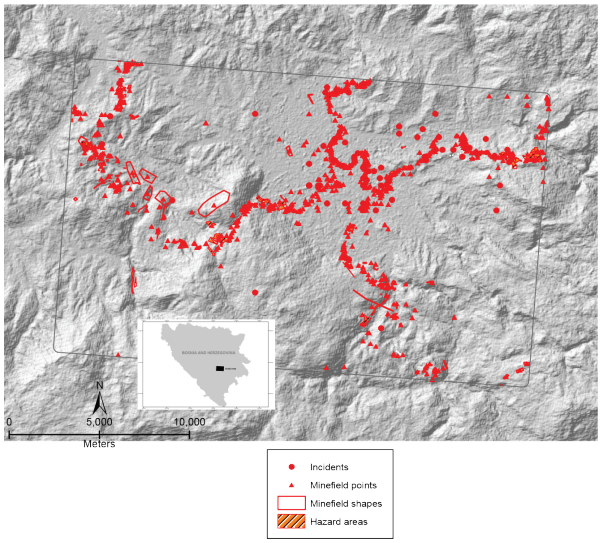


**Figure 3:** Hadzici study area in Bosnia and Herzegovina.

The set of explanatory variables used in this study, consist of land-cover data (forest, pasture, cultivated, built-up area, shrubs, bare soil, water bodies), topographic data (elevation and hill-slope gradient), and a group of indirect indicators such as land-use changes and other infrastructure data, specific to each case study. For the KDE analysis and visualization, the used variables are listed in Tables 2 and 3, for the two considered study areas, respectively. For the risk analysis, the used variables are listed in Tables 4 and 5. The categorical variables have been obtained as follows: (i) for the considered variable (line or polygon border of the analysed feature), we first create a raster map defining for each cell the minimal distance to the considered variable; and (ii) the distances are then grouped with natural-breaks into five distance-based classes.

## Kernel density estimation

**Dolac region:** As explained in Section 6.2.1, we calculated a KDE map that includes both, the original point data and other point locations representing the polygon-shaped mine fields and hazard areas. In this section, we illustrate the KDE results using the Dolac data. First, an adaptive KDE-based map is obtained using only the incident and mine field point data. In this map, the optimal pilot bandwidth is 332.6 m. Once the map is classified (on a five natural-break-based classification), the higher risk class is found to be characterized by incidents and minefield points density of 19.6 point locations per square kilometre. Thus, random points following such a density are generated over the polygon-shaped mine action data. Figure 4 shows the final adaptive KDE-based map obtained using an optimal bandwidth of 348.7 m. The resulting map highlights one very-high density sub-zone at the North-East of the study area, surrounded by a sub-region of high density. There is also another high-density sub-zone in the South-West of the study area. Those areas can be chosen as priorities for further land release tasks (non-technical/technical survey and clearance). The figure also shows that the region designed as confirmed or suspected hazard area by BHMAC overlaps the predicted hazard obtained using KDE. This indicates that a KDE map calculated in the way we propose in this paper, can provide a preliminary prediction of landmines and ERW-related risk areas.

To illustrate the importance of using an adaptive bandwidth, we show in Figure 5 the KDE map generated using a fixed bandwidth. The optimal fixed bandwidth for all the points in this map was selected with the leave-one-out LSCV method [50]. Visual inspection allows to observe that all density levels have a wider extent than in the adaptive bandwidth-based map, as the bandwidth does not take into account the relative distance of the neighbours at each location point.

Overlaying KDE results on topographic data (elevation) and transport facilities as illustrated in Figure 6, one can notice a high-density of landmine and ERW risk in the South-West part of the study region, corresponding to a low altitude area near a road and railway. However, the high-risk zone of the NorthEast area is hilly with few tracks. Thus, we can infer two different landmines and ERW emplacement strategies: a blocking strategy to prevent the mobility of people, and a defensive strategy for observation and dominance. This is also confirmed in Figure 7 illustrating the land-cover type corresponding to the high-risk areas.

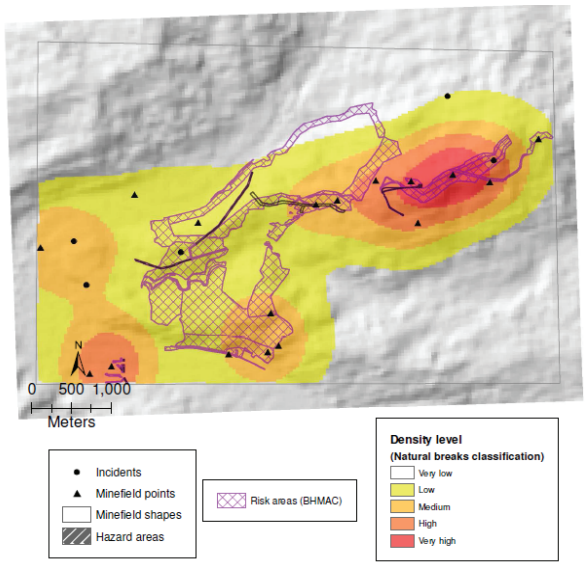


**Figure 4:** Dolac: kernel density estimation.

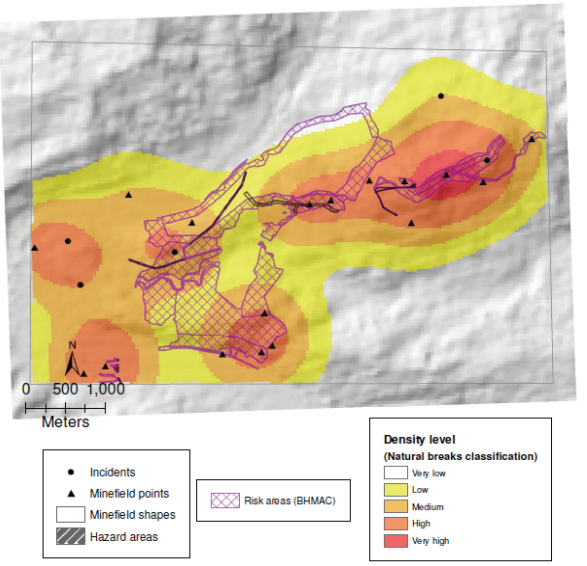


**Figure 5:** Dolac: kernel density estimation using a fixed bandwidth.

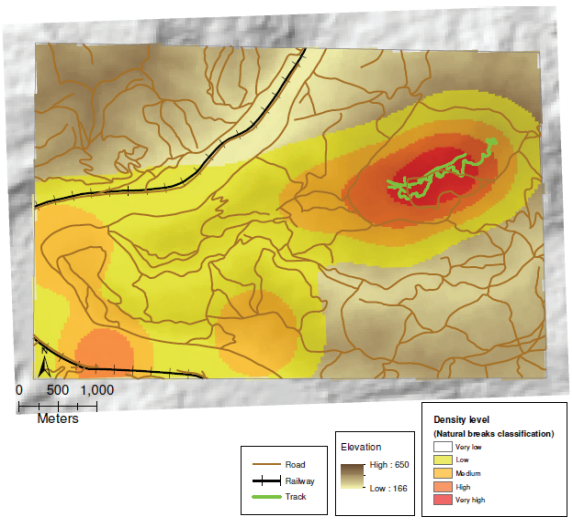


**Figure 6:** Dolac: kernel density estimation overlay on topographic and transport Facilities.

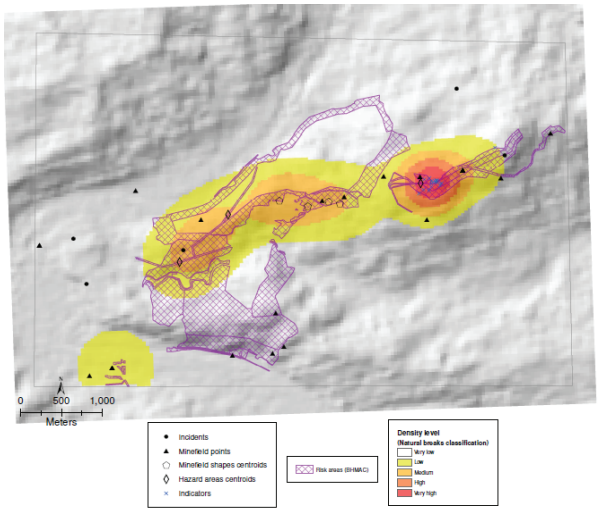


**Figure 8:** Dolac: kernel density estimation for mine action data (including online-generated random points for mine field polygons and hazard areas) and risk indicators generated using an adaptive bandwidth.

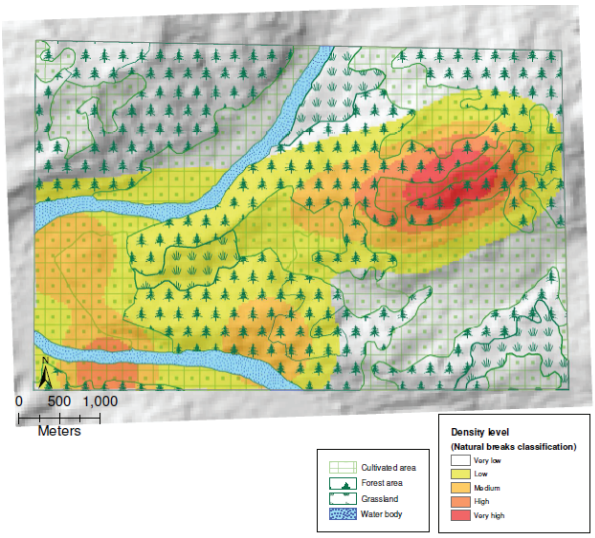


**Figure 7:** Dolac: kernel density estimation visualized together with land-cover types.

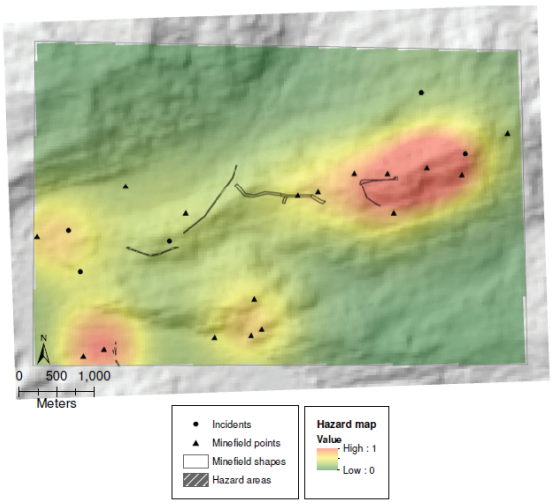


**Figure 9:** Dolac: hazard map.

Combining the mine action data with landmine and ERW risk indicators defined in the Table 2, we obtain the KDE map of Figure 8. By comparing Figures 4 and 8, one can notice that using the risk indicators as evidence of hazard, allows reducing the risk area and highlights the middle area of the study zone with a better overlap on the hazard area, defined as confirmed or suspected by BHMAC.

## Disaster risk analysis

**Dolac region:** For the Dolac region, we estimated the hazard map as illustrated in Figures 9 and 10, obtained using the mine action data. The element-at-risk layer for this study area was estimated using as parameter the distance to cultivated areas represented as categorical variable as shown in Figure 11. The obtained element-at-risk map weighted according to Equation (5) is presented in Figure 12.

The final risk map is given in Figure 13. It highlights very-high to medium risk zones for the cultivated areas (Figure 14) where high landmine and ERW contamination is observed. Such map can be used along with the risk map produced by BHMAC or the hazard map of Figure 9 to prioritize the land release activities in high risk areas affecting access to agriculture areas.

**Hadzici region:** Figures 15-18 present the results for each one of the three intermediate maps used for the risk analysis in the Hadzici study area. Figure 15 illustrates the hazard map obtained using KDE applied to the mine action data and landmine and ERW risk indicators of the Table 5. The vulnerability analysis (Figure 16) presents the combined result of taking into account both, the presence of buildings and increased vegetation zones according to the intermediate dual KDE maps.

The element-at-risk layer for this study area was estimated using as parameter the distance to built-up areas represented as categorical variables as shown in Figure 17. The obtained element-at-risk map

| Variable | Type | Source |
|---|---|---|
| **Response (dependent)**<br>Incidents and mine field points | points | BHMAC |
| Mine field polygons and hazard areas | polygons | BHMAC |
| Landmines and ERW risk indicators Craters and holes | points | SAFEDEM-DEMO |
| Potential risk areas Risk areas | polygons | BHMAC |
| **Analysis variables (independent)**<br>Land-cover and land-use | polygons | CLC EEA-based |
| Roads | lines | BHMAC |
| Railways | lines | BHMAC |
| Tracks | lines | SAFEDEM-DEMO |
| Topographic Elevation | continuous | ASTER GDEM |

**Table 2:** Variables used for KDE analysis in the Dolac study area.

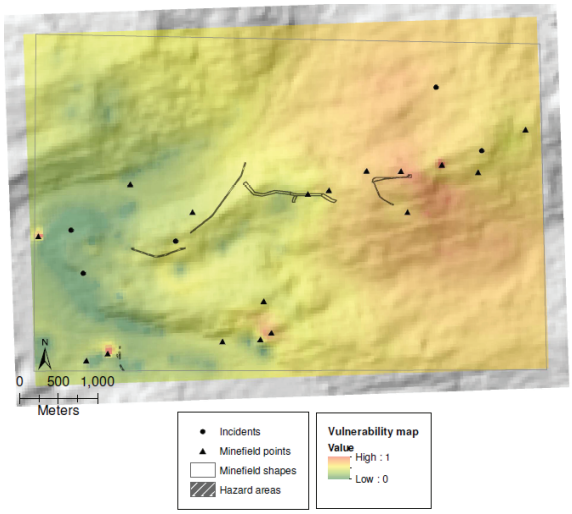


**Figure 10:** Dolac: vulnerability map.

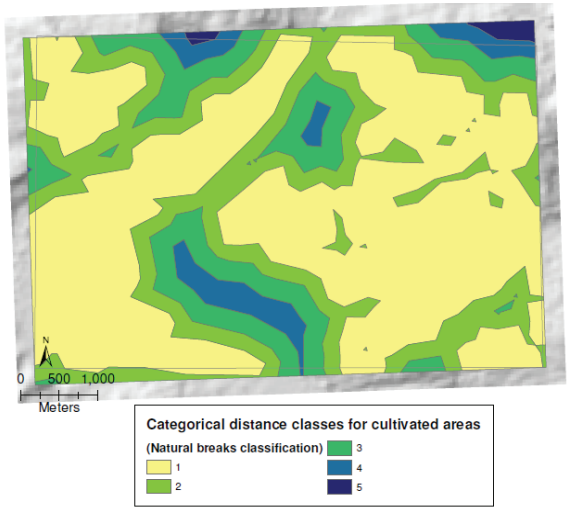


**Figure 11:** Hadzici: categorical classes for agriculture areas.

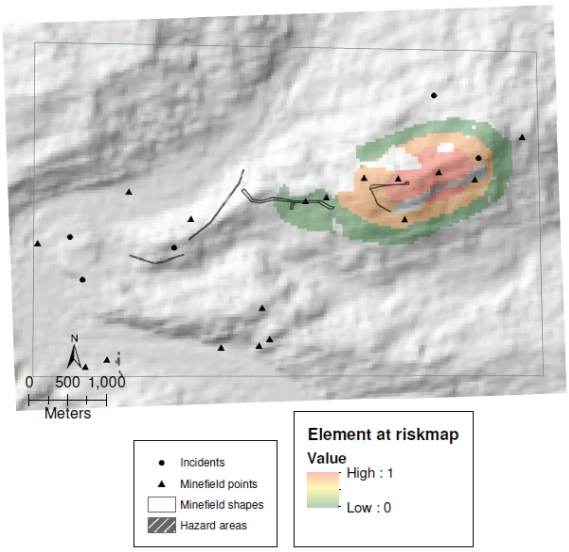


**Figure 12:** Dolac: element-at-risk map.

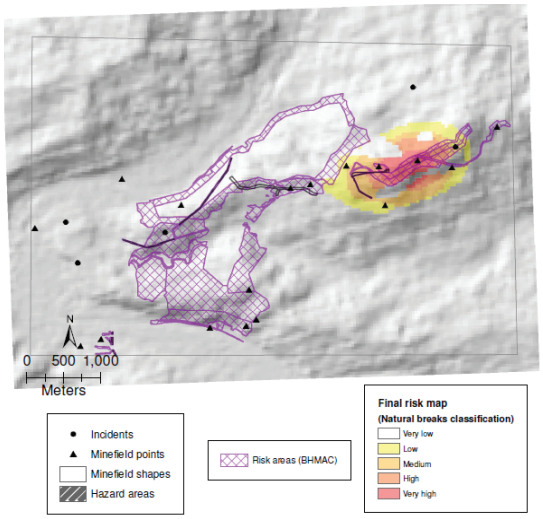


**Figure 13:** Dolac: final risk map versus con_rmed risk area by BHMAC.

weighted according to Equation (5) is presented in Figure 18. The final risk map shown in Figure 19 highlights the built-up areas more affected by very-high to medium risk zones (Figure 14), where high landmine and ERW contamination is observed. As illustrated in Figure 20, other very high and high risk zones overlap with several roads, showing how landmines and ERW are used as a blocking strategy to prevent the mobility of people. Together with the risk map produced by BHMAC, this risk analysis can be used to prioritize the land release activities in risk areas affecting the population safety and mobility.

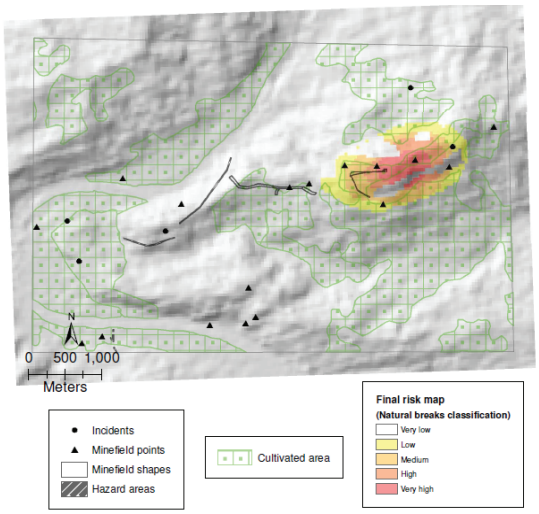


**Figure 14:** Dolac: final risk map overlaid on the land-cover type cultivated areas.

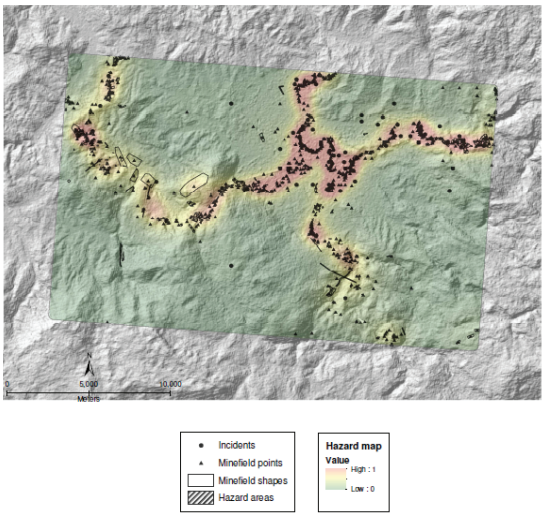


**Figure 15:** Hadzici: hazard map.

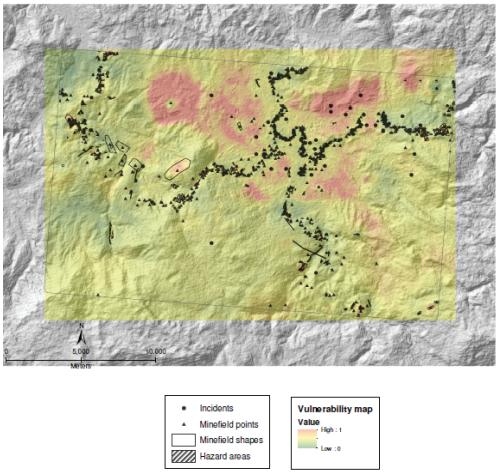


**Figure 16:** Hadzici: vulnerability map.

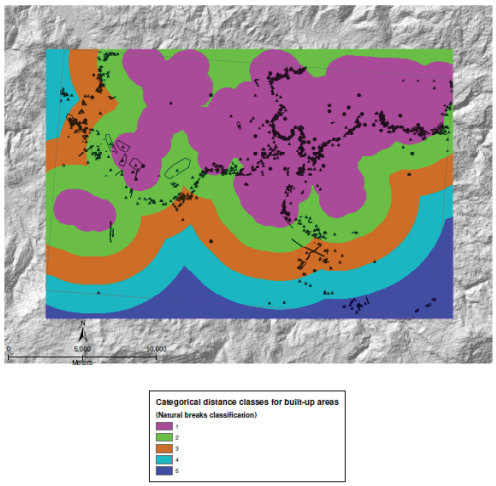


**Figure 17:** Hadzici: categorical classes for built-up areas.

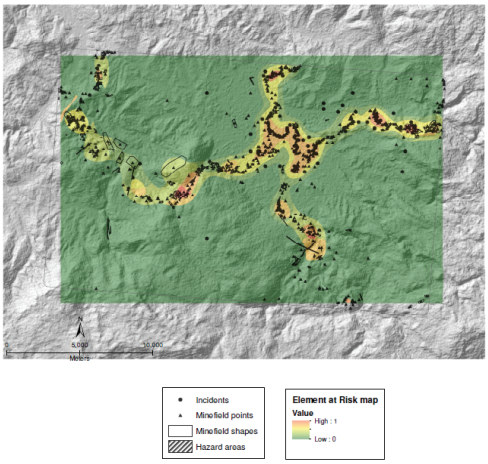


**Figure 18:** Hadzici: element-at-risk map.

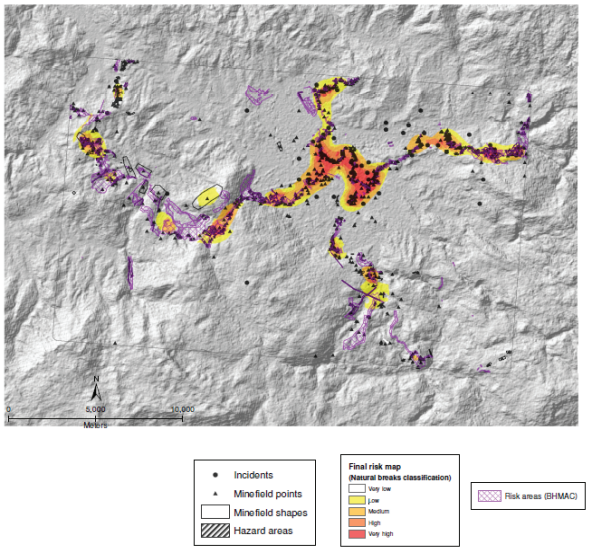


**Figure 19:** Hadzici: _nal risk map overlaid with risk areas (BHMAC).

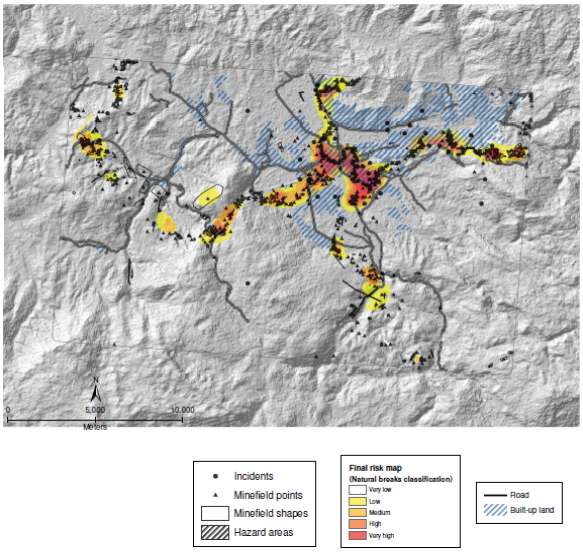


**Figure 20:** Hadzici: final risk map overlaid with built-up areas and roads.

| Variable | Type | Source |
|---|---|---|
| **Response (dependent)** Incidents and mine field points | points | BHMAC |
| Mine field polygons and hazard areas | polygons | BHMAC |
| Landmines and ERW risk indicators Building ruins and other indicators | points | SAFEDEM-SADA |
| Potential risk areas Risk areas | polygons | BHMAC |
| **Analysis variables (independent)** Topographic Elevation | continuous | ASTER GDEM |

**Table 3:** Variables used for KDE analysis in the Hadzici study area.

| Variable | Type | Source |
|---|---|---|
| **Response (dependent)** Incidents and mine field points | points | BHMAC |
| Mine field polygons and hazard areas | polygons | BHMAC |
| **Predictor (independent)** Distance to cultivated areas | categorical | CLC EEA-based |
| Buildings | points | BHMAC |
| Craters and holes | point | SAFEDEM-DEMO |

**Table 4:** Variables used for Disaster Risk analysis in the Dolac study area.

| Variable | Type | Source |
|---|---|---|
| **Response (dependent)** Incidents and mine field points | points | BHMAC |
| Mine field polygons and hazard areas | polygons | BHMAC |
| Landmines and ERW risk indicators Building ruins and other indicators | points | SAFEDEM-SADA |
| **Predictor (independent)** Distance to built-up areas | categorical | CLC EEA-based |
| Buildings | points | SAFEDEM-SADA |
| Centroids of areas showing vegetation gain | points | SAFEDEM-SADA |

**Table 5:** Variables used for Disaster Risk analysis in the Hadzici study area.

## Conclusions

This paper uses geo-spatial analysis to provide insight into potential landmine and Explosive Remnants of War (ERW) risk areas based on a set of environmental features. The study demonstrates that adaptive-bandwidth Kernel Density Estimation (KDE) can be used not only as a landmine and ERW contamination measure, but also as the basis for disaster risk analysis, as commonly defined, namely a combination of hazard, vulnerability and element at risk components. To extend the use of KDE to polygon-shaped data, we propose a new infilling method for polygons. This approach proves convenient for landmine and ERW contamination evaluation.

Our risk analysis approach is mainly based on an original variant of the use of the KDE method. Indeed, the hazard component identifies areas where landmine and ERW hazards are likely to occur, according to an adaptive-bandwidth KDE map. The dual KDE is used to estimate the vulnerability component of the risk. Additionally, the chosen element-at-risk component is weighted according to the three-top natural-breaks based classification of the KDE map.

Our method is tested on two different study areas in BIH. It enabled the discovery of zones where the chosen element at risk is more affected. On the Dolac study area, the final risk map helps to prioritize the land release activities in high risk areas affecting access to agriculture zones, already designated as risky by the Bosnia and Herzegovina Mine Action Centre (BHMAC). The results on the Hadzici study area are validated by a good match against the overlaying risk regions designated as confirmed and suspected by BHMAC. They highlight population blocking in built-up zones and roads on specific places. It also draws attention to the potential danger on some few unexplored areas depicted as being under medium risk. Thus, the method proposed in this feasibility study can be used as a strategy in humanitarian mine action reducing time and cost of choosing priority areas for land release.

### Acknowledgements

This work has been conducted within the framework of the ESA IAP ARTES 20 SAFEDEM Demonstrator Project with the financial support of BELSPO and VUB.

### References

1. International Campaign to Ban Landmines (2015) Landmine Monitor 2015.
2. Mitchell SK (2004) Death, disability, displaced persons and development: the case of landmines in Bosnia and Herzegovina. World Development 32: 2105-2120.
3. Varnes DJ (1984) Landslide hazard zonation: a review of principles and practice. UNESCO Press, Paris.
4. Van Westen CJ, Castellanos E, Kuriakose SL (2008) Spatial data for landslide susceptibility, hazard, and vulnerability assessment: an overview. Engineering geology 102: 112-131.
5. United Nations Mine Action Service (2003) IMAS 04.10 Glossary of mine action terms, definitions and abbreviations - Amendment 7.
6. United Nations Mine Action Service (2009) IMAS 07.11 Land Release - Amendment 2.
7. Maathuis B (2002) Remote sensing based detection of landmine suspect areas and minefields. PhD Thesis, International Institute for Aerospace Survey and Earth Sciences (ITC).
8. Maathuis BHP, Genderen JV (2004) A review of satellite and airborne sensors for remote sensing based detection of minefields and landmines. International Journal of Remote Sensing 25: 5201-5245.
9. Katartzis A, Vanhamel I, Chan JCW, Sahli H (2004) Remote sensing minefield area reduction: Model-based approaches for the extraction of minefield indicators. In: Theory and Applications of Knowledge-Driven Image Information Mining with Focus on Earth Observation 553: 18.
10. Chan JCW, Sahli H, Wang Y (2005) Semantic risk estimation of suspected minefields based on spatial relationships analysis of minefield indicators from multi-level remote sensing imagery. In Defense and Security, International Society for Optics and Photonics, pp: 1071-1079.
11. Chan JW, Alegria AC, Veratelli MG, Folegani M, Sahli H (2012) Combined spatial point pattern analysis and remote sensing for assessing landmine

affected areas. In Geoscience and Remote Sensing Symposium (IGARSS), 2012 IEEE International, pp: 5368-5371.

12. Schultz C, Alegría AC, Cornelis J, Sahli H (2016) Comparison of spatial and a spatial logistic regression models for landmine risk mapping. Applied Geography 66: 52-63.
13. Silverman BW (1986) Density estimation for statistics and data analysis. CRC Press, Florida, USA.
14. Charpentier A, Gallic E (2016) Kernel density estimation based on Ripley's correction. GeoInformatica 20: 95-116.
15. Tobler WR (1970) A computer movie simulating urban growth in the Detroit region. Economic Geography 46: 234-240.
16. Ramanna CK, Dodagoudar GR (2012) Seismic hazard analysis using the adaptive kernel density estimation technique for Chennai city. Pure and Applied Geophysics 169: 55-69.
17. Eck J, Chainey S, Cameron J, Wilson R (2005) Mapping crime: understanding hot spots. Report, USA: National Institute of Justice.
18. Rushton G (2003) Public health, GIS, and spatial analytic tools. Annual Review of Public Health 24: 43-56.
19. Feuillet T, Charreire H, Menai M, Salze P, Simon C, et al. (2015) Spatial heterogeneity of the relationships between environmental characteristics and active commuting: towards a locally varying social ecological model. International Journal of Health Geographics 14: 1-14.
20. Lewis T, Bennett S (2013) The juxtaposition and spatial disconnect of environmental justice declarations and actual risk: A new method and its application to New York State. Applied Geography 39: 57-66.
21. Kenchington E, Murillo FJ, Lirette C, Sacau M, Koen-Alonso M, et al. (2014) Kernel density surface modelling as a means to identify significant concentrations of vulnerable marine ecosystem indicators. PloS ONE 9: e109365.
22. Worton BJ (1987) A review of models of home range for animal movement. Ecological Modelling 38: 277-298.
23. Lees KJ, Guerin AJ, Masden EA (2016) Using kernel density estimation to explore habitat use by seabirds at a marine renewable wave energy test facility. Marine Policy 63: 35-44.
24. Alegría AC, Sahli H, Zimányi E (2011) Application of density analysis for landmine risk mapping. In: Spatial Data Mining and Geographical Knowledge Services (ICSDM), 2011 IEEE International Conference on IEEE, pp: 223-228.
25. Lacroix P, Herzog J, Eriksson D, Weibel R (2013) Methods for visualizing the explosive remnants of war. Applied Geography 41: 179-194.
26. Duong T (2004) Bandwidth selectors for multivariate kernel density estimation. University of Western Australia, Crawley, Australia.
27. Li Q, Racine JS (2007) Nonparametric econometrics: theory and practice. Princeton University Press, New Jersey, USA.
28. Scott DW (2015) Multivariate density estimation: theory, practice, and visualization. John Wiley & Sons, New Jersey, USA.
29. Wand MP, Jones MC (1994) Kernel smoothing. CRC Press, Florida, USA.
30. Lemke D, Mattauch V, Heidinger O, Pebesma E, Hense HW (2015) Comparing adaptive and fixed bandwidth-based kernel density estimates in spatial cancer epidemiology. International Journal of Health Geographics 14: 15.
31. Davies TM, Hazelton ML, Marshall JC (2011) Sparr: analyzing spatial relative risk using fixed and adaptive kernel density estimation in R. Journal of Statistical Software 39: 1-14.
32. Abramson IS (1982) On bandwidth variation in kernel estimates-a square root law. The Annals of Statistics 10: 1217-1223.
33. Oviasu OI (2015) Using a dual kernel density estimate as a preliminary evaluation of the spatial distribution of diagnosed chronic kidney disease (CKD) in Edo State, Nigeria. Geo Journal 80: 711-720.
34. Larsen MA (2010) Philadelphia traffic accident cluster analysis using GIS and SANET. Master of Urban Spatial Analytics Capstone Project.
35. Levine N (1999) CrimeStat: a spatial statistics program for the analysis of crime incident locations. In Proc. of the 4th Int. Conf. on Geocomputation. Mary Washington College, Virginia, USA.
36. Walker WC, Sim S, Keys-Mathews L (2014) Use of geographically weighted regression on ecology of crime, response to hurricane in Miami, Florida. Forensic GIS 11: 245-262.
37. Kelsall JE, Diggle PJ (1995) Non-parametric estimation of spatial variation in relative risk. Statistics in medicine 14: 2335-2342.
38. Cowie AP (2002) Harmonising the vocabulary of risk. In: Proceedings of the Tenth EURALEX International Congress, EURALEX 2002: Copenhagen, Denmark, pp: 325-330.
39. Ahmed A (2014) GIS and Remote Sensing for Malaria Risk Mapping, Ethiopia. The International Archives of Photogrammetry, Remote Sensing and Spatial Information Sciences 40: 155-161.
40. Upadhyay V, Jat MK (2014) Risk assessment of petroleum fire using geospatial techniques. International Journal of Remote Sensing and Geoscience 3: 11-20.
41. Müller M, Vorogushyn S, Maier P, Thieken AH, Petrow T, et al. (2006) CEDIM Risk Explorer? a map server solution in the project "Risk Map Germany". Natural Hazards and Earth System Science 6: 711-720.
42. Gaprindashvili G, Van Westen CJ (2016) Generation of a national landslide hazard and risk map for the country of Georgia. Natural Hazards 80: 69-101.
43. United Nations International Strategy for Disaster Reduction (2009) Terminology on disaster risk reduction.
44. Jenks GF (1967) The data model concept in statistical mapping. International Yearbook of Cartography 7: 186-190.
45. United Nations International Strategy for Disaster Reduction (2004) Living with risk: a global review of disaster reduction initiatives. United Nations Publications, New York, USA.
46. Glade T (2003) Vulnerability assessment in landslide risk analysis. Die Erde 134: 123-146.
47. Torun A, Düzgün S (2006) Using spatial data mining techniques to reveal vulnerability of people and places due to oil transportation and accidents: a case study of Istanbul strait. In: ISPRS Technical Commission II Symposium, Vienna, pp: 12-14.
48. Rapicetta S, Zanon V (2009) GIS-based method for the environmental vulnerability assessment to volcanic ashfall at Etna Volcano. GeoInformatica 13: 267-276.
49. Bosnia and Herzegovina Mine Action Centre (2014) Bosnia and herzegovina mine action report 2013. Report, Bosnia and Herzegovina Mine Action Centre.
50. Bowman AW, Azzalini A (1997) Applied smoothing techniques for data analysis: the kernel approach with S-Plus illustrations: the kernel approach with S-Plus illustrations. Oxford University Press, Oxford, England, UK.